Influence of Transition Metal Additives on the Hydriding/Dehydriding Critical Point of $NaAlH_4$

C. K. Huang,[†] Y. J. Zhao,[†,‡] T. Sun,[†] J. Guo,[§] L. X. Sun,[||] and M. Zhu*[,†]

School of Materials Science and Engineering, South China University of Technology, Guangzhou 510640, P. R. China, Department of Physics, South China University of Technology, Guangzhou 510640, P. R. China, College of Physics Science and Technology, Guangxi University, Nanning 530004, P. R. China, and Dalian Institute of Chemical Physics, Chinese Academy of Science, Dalian 116023, P. R. China

Received: October 4, 2008; Revised Manuscript Received: March 29, 2009

The influence of transition metals (TMs) on the hydriding/dedydriding critical point of $NaAlH_4$ has been studied using the chemical potential method. The theoretical results predict that, if the reaction system reaches equilibrium, most of the TM additives significantly increase its hydriding/dedydriding critical point in the sequence Pd > Co > Zr > Ni > Nb > Hf > Ti > Mn > Fe > V > Cu > Cr and therefore have destabilizing effects on $NaAlH_4$ in the same sequence. Experimentally, the isothermal dehydriding kinetics of $NaAlH_4$ is studied only with Fe, Ti, and FeTi additives. The experimental results show that the destabilizing effect of Fe and Ti additives with coarse particles is very low while more effective destabilizing ability is achieved with fine FeTi particles. These experimental results suggest that the predicted destabilizing effect of TM additive is hindered kinetically due to the coarse particles of additives, and therefore experimental verification of the destabilizing effect of TMs should be performed with nanosized particles.

1. Introduction

Hydrogen is one of the most promising energy carriers and is expected to replace fossils fuels as the dominating energy source in the future. However, getting effective hydrogen storage materials is one of the bottlenecks for using hydrogen energy. For instance, the well-developed AB_5 alloys have a low hydrogen storage capacity of only 1.5 wt %.[1,2] In order to get higher storage capacity, light element containing materials have been targeted as candidates. Unfortunately, those materials are generally poor in hydrogen absorption/desorption kinetics. For example, Mg has a theoretical hydrogen storage capacity up to 7.6 wt %, while it needs a relatively high temperature for dehydriding and the kinetic property is very poor.[3,4] The RE−Mg−Ni systems have been brought forward to overcome the shortcomings of AB_5 and Mg-based hydrogen storage alloys; however, the result is still not satisfactory.[5,6] The complex hydrides have high gravimetric and volumetric hydrogen storage densities but had not realized reversible hydrogen absorption and desorption under moderate temperature and H_2 pressure conditions until a breakthrough was made in 1997 by Bogdanovic et al.[7] They showed that the reaction kinetics of $NaAlH_4$ can be greatly improved by adding $TiCl_3$ as a catalyst. Their work initiated great effort in exploring complex hydrides for hydrogen storage, and one of the major concerns is how to select suitable additives which can catalyze the hydrogen absorption/desorption kinetics of complex hydrides effectively.

In recent years, the catalytic effect of different dopants on dehydriding reaction of $NaAlH_4$ has been investigated. Zidan[8] et al. reported that Zr is inferior to Ti as a catalyst for the dehydriding of $NaAlH_4$ to Na_3AlH_6 but superior to the dehydriding of Na_3AlH_6 to NaH. It was reported that Sc,[9] Hf,[10] V,[11] and rare earth compounds[12,13] can also catalyze dehydriding of complex hydrides. Although the catalytic mechanism of those compounds remains unclear,[14−18] there is a common understanding that the cations have more remarkable catalytic effect than the anions. It has been noted that the particle size of catalyst is also an important factor. Fichtner et al.[19] found that the Ti_{13}·6 THF nanoparticles, in which the Ti valence is zero, have a better catalytic effect than $TiCl_3$, and they considered that the key of the activity is the nanoscale size of the particles. Similarly, Bagdanovic[20] found that Ti·0.5 THF cluster had better catalytic effect than $TiCl_3$. Kang et al.[21] synthesized $NaAlH_4$ by milling NaH powders with Al and Ti powders under hydrogen atmosphere and found that the system had better kinetics than that obtained by adding Ti to $NaAlH_4$ directly.

Many researches have conducted first-principles calculations to study the catalytic mechanism of TM to $NaAlH_4$ with major attention to the effect of transition metal atoms (usually referred to as defects).[22−24] The effect of 3d TM defects in crystalline $NaAlH_4$ was studied by Blomqvist et al.[22] They revealed that doped atoms tend to bond with nearby Al atoms, which decreases the bond strength of Al−H and results in an easier release of hydrogen. They also showed that Cr and Fe defects have a better effect than Ti defect in $NaAlH_4$. The (001) and (100) surfaces of $NaAlH_4$ with Ti defect have also been investigated based on the slab model by Liu et al.[23] A local structure formed in both surfaces with a formula of $TiAl_3H_{12}$, which is a precursor state of $TiAl_3$. The hydrogen desorption energy decreases considerably from the $TiAl_3H_{12}$ complex in comparison with that of undoped clean $NaAlH_4$ surfaces. Marashdeh et al.[24] carried out calculations by the cluster approach and found that some Ti−Al−H local complexes were

* Corresponding author. Tel.: (+86) 020-87113924. Fax: 020-87111317. E-mail address: memzhu@scut.edu.cn.
[†] School of Materials Science and Engineering, South China University of Technology.
[‡] Department of Physics, South China University of Technology.
[§] Guangxi University.
[||] Chinese Academy of Science.

10.1021/jp808775v CCC: $40.75
Published on Web 05/07/2009

favorable with existence of Ti defect, which is similar to the results calculated with the slab model.[23]

To improve the kinetic performance of complex hydrides, it is important to find appropriate additives. It is reported in experiments that additives not only have catalyzing effect but also thermodynamic destabilizing effect to the complex hydrides. In general, when an additive is added to a complex hydride, some new compound phases may form after reactions. For instance, when $NaAlH_4$ is doped with $TiCl_3$, NaCl and Ti−Al alloys form during the decomposition of $TiCl_3$.[16,17] The thermodynamic equilibrium relation of the reaction system would alter with the formation of new phases related to additives. Therefore, the hydriding/dehydriding equilibrium hydrogen pressure, $P^{eq}_{H_2}(T)$, the characteristic parameter of hydriding/dehydriding equilibrium reaction systems, would shift, which is known as destabilization.[25−27] Thus, it is also important to evaluate the effect of additives in thermodynamic aspects for exploring better additives. However, the destabilization problem has not been extensively studied by phase equilibrium theory yet. In this work, we try to study the hydridng/dehydriding thermodynamics of $NaAlH_4$ with equilibrium phase theory. Experiments were conducted with Fe, FeTi, and Ti-doped $NaAlH_4$ to compare with the theoretical predictions.

2. Theoretical and Experimental Method

2.1. Theoretical Approaches. In this work, we simply adopt the global equilibrium approach. The character of this state is that the chemical potential of a component is equal everywhere in the system. Besides, it neglects all the kinetic barriers reaching equilibrium state. Therefore, it is very convenient to characterize equilibrium state with chemical potentials, and the equilibrium phase diagram can be characterized by chemical potential with the following two benefits:

The first is that the hydriding/dehydriding critical point can be determined directly by the intersection point of some phase boundaries with the lowest chemical potential of hydrogen. Here, the hydriding/dehydriding critical point corresponds to an equilibrium state in which the atomic chemical potentials in the reactant are equal to those in the products. The critical point can be described by $\mu^{eq}_H(T)$. It is well-known that the relation of temperature and pressure satisfy the Van't Hoff's law at critical points. Hydriding or dehydriding reaction should take place, respectively, when the environmental chemical potential of hydrogen $\mu_H(T)$ is higher or lower than $\mu^{eq}_H(T)$ at temperature T. When studying the situation beyond 0 K, one needs to consider the free energy changes due to entropy, vibrational/translational/rotational motion of the solid phases, and H_2 in the reaction system, as discussed by S. V. Alapati et al.[28] However, the calculations of vibration entropy and vibration energy in solids require phonon calculations, which will require huge computational resources. Here, we only discuss the critical point at 0 K in order to study the destabilizing effect of TM different additives.

The second benefit is that under the hydriding/dehydriding equilibrium state, $\mu^{eq}_H(T)$ has a quantitative relation, as given in eq 1, with the equilibrium hydriding/dehydriding H_2 pressure, $P^{eq}_{H_2}(T)$, which makes it possible to compare theoretical result with experiment.

$$2\mu^{eq}_H(T) = \mu^{eq}_{H_2}(T) = \mu^0_{H_2} + RT\ln[P^{eq}_{H_2}(T)] \qquad (1)$$

Generally, the hydriding/dehydriding critical point is determined by both temperature and chemical environment. To compare with experiment, it is much better to calculate the hydriding/dehydriding critical point under the conditions corresponding to experiment. However, the temperature effect is hard to handle in the first-principles calculation. Fortunately, it is well-known that the 0 K approximation is a good approximation [22−24,33] for the enthalpies of most solid state materials. For a semiquantitative comparison, here in this work, the destabilizing ability of TMs to $NaAlH_4$ was studied with 0 K approximation, which will not change the order of destabilizing ability to $NaAlH_4$ for the studied TM additives.

At 0 K, for a crystal compound of A_mB_n in a reaction system under equilibrium, its formation enthalpy, $H_f(A_mB_n)$, can be characterized by the chemical potential of its components

$$H_f(A_mB_n) \quad \underline{\text{at 0 K}} \quad G(A_mB_n) = m\mu_A + n\mu_B \qquad (2)$$

Here μ_A and μ_B are the absolute chemical potential of an element A and B, respectively, in a certain chemical environment, and $H_f(A_mB_n)$ can be obtained by eq 3.

$$H_f(A_mB_n) = E(A_mB_n) - mE(A) - nE(B) \qquad (3)$$

where $E(A_mB_n)$, $E(A)$, and $E(B)$ are total energy of A_mB_n, A, and B in their crystalline state. In the calculation of the total energy, we adopted crystalline state approximations, i.e., assuming the structure of all the phases satisfy periodical boundary conditions.

In this work the first-principles method was used to analyze the hydriding/dehydriding critical point of $NaAlH_4$ with and without TM additives under the above three approximations, global equilibrium, 0 K, and crystalline state approximations. By this method, we try to explain the destabilizing mechanism as well as the semiquantitative relation of TMs additives on the critical point of $NaAlH_4$ reported by many previous experiments.

2.2. Computational Method. The total energies in eq 3 were calculated with the CASTEP program[29] based on density functional theory[30,31] and plane-wave pseudopotential method. We used ultrasoft pseudopotential to describe the atomic potentials and used the PW91 formulism of generalized gradient approximation[32] for exchange correlation functional. Spin-polarization is considered in Ni, Co, Fe, and their compounds. Brillouin zone was sampled with the *K*-points generated by the *k*-mesh with a distance less than 0.03 $Å^{-1}$ in the reciprocal space, and the cutoff energy was set to 420 eV. Structural relaxations were converged to 0.01 eV/Å for the residual forces. The formation enthalpy of $FeAl_{3.2}$ is calculated by a linear interpolation to $Fe_{12}Al_{37}$ and $Fe_{12}Al_{39}$.

2.3. Experimental Method. To compare the theoretical results with the experiment, Fe, Ti, and FeTi were doped into $NaAlH_4$, respectively, by ball milling (BM), which is the most commonly used method to add catalysts in complex hydrides now. The $NaAlH_4$ powders with purity of 95% were purchased from Sigma-Aldrich Corp. The Ti and Fe powders had purity of 99.9% and 200 mesh size. The FeTi alloy powders were synthesized by BM. The milling was performed in a QM-3A vibratory mill using a stainless vial and grinding balls, and the ratio of ball to powder was 10:1. All the handling of specimens was performed in the glovebox under high pure argon (99.99%) atmosphere and with the content of water and oxygen less than 3 ppm. A LEO 1530 VP scanning electron microscope was used to characterize the distribution of dopants in $NaAlH_4$. Isothermal dehydrogenation properties at 393 K were examined in a gas reaction controller made by Advance Materials Corporation with the starting H_2 pressure of 10 MPa. The isothermal dehydrogenation kinetic curve of pure $NaAlH_4$ was given as reference to compare the destabilizing effect of TMs additives to $NaAlH_4$,

TABLE 1: Formation Enthalpies of $NaAlH_4$, Na_3AlH_6, AlH_3, NaH, and Stable Ti-Containing Compounds

	formation enthalpies		
	this work	experimental	
phase	(eV/f.u.)	(kJ·mol^{-1})	(eV/f.u.)
$NaAlH_4$	−1.06	−113[a]	−1.17
Na_3AlH_6	−2.10		
AlH_3	−0.18	−11.401[b]	−0.12
NaH	−0.43	−56.442[b]	−0.58
TiH_2	−1.55	−144.384[b]	−1.50
$TiAl_3$	−1.59	−146.440[b]	−1.52
Ti_3AlH[c]	−1.91		

[a] Reference 33. [b] Reference 35. [c] Reference 36. All the experimental data are attained in a standard state of 298.15 K and 1 bar. All the estimated uncertainties to the calculated results in this paper are 0.01 eV.

avoiding the influence of BM on the hydriding/dehydriding critical point.

3. Results and Discussion

3.1. The Equilibrium Phase Diagram of $NaAlH_4$ Characterized with Chemical Potentials. The Na−Al−H system is used to illustrate how to characterize an equilibrium phase diagram by the chemical potential approach. All the known possible binary and ternary phases in the Na−Al−H system are listed in Table 1, which were searched from the available databases, such as ICSD and ACS. The formation enthalpies of those phases calculated in this work and reported by others from experiment measurements are also given in Table 1.

When the chemical potential of elemental A in its perfect crystal, μ_A^{crys}, is adopted as the reference, the relative chemical potential of element A is denoted as $\Delta\mu_A = \mu_A - \mu_A^{crys}$. According to the definition given before, the relative chemical potentials of the Na, Al, and H are denoted as the following: $\Delta\mu_{Na} = \mu_{Na} - \mu_{Na}^{crys}$, $\Delta\mu_{Al} = \mu_{Al} - \mu_{Al}^{crys}$, and $\Delta\mu_H = \mu_H - (1/2)\mu_{H_2}^{gas}$.

The equilibrium condition of single phase $NaAlH_4$ is given in eq 4.

$$\Delta\mu_{Na} + \Delta\mu_{Al} + 4\Delta\mu_H = H_f(NaAlH_4) \quad (4)$$

To avoid the formation of the elemental Na, Al crystal, and H_2 molecule, the chemical potentials should satisfy

$$\Delta\mu_{Na} \le 0,\ \Delta\mu_{A1} \le 0,\ \Delta\mu_H \le 0 \quad (5)$$

Furthermore, other binary and ternary phases must also be excluded to keep $NaAlH_4$ stable. To avoid the formation of Na_3AlH_6, AlH_3, and NaH phases, the following chemical potential relationship should be satisfied

$$3\Delta\mu_{Na} + \Delta\mu_{Al} + 6\Delta\mu_H \le H_f(Na_3AlH_6) \quad (6)$$

$$\Delta\mu_{Al} + 3\Delta\mu_H \le H_f(AlH_3) \quad (7)$$

$$\Delta\mu_{Na} + \Delta\mu_H \le H_f(NaH) \quad (8)$$

From the confining conditions given in eqs 4−8, the equilibrium phase diagram characterized by chemical potential without additive can be obtained and is shown in Figure 1. The shadowed area in Figure 1 corresponds to the $NaAlH_4$ stable chemical potential region (SCPR). In principle, hydrogen is released when the chemical potential of H in the environment is smaller than that in solid until a multiphase equilibrium environment is reached. The hydriding/dehydriding critical point is the intersection of the phase boundaries with lowest $\Delta\mu_H$,

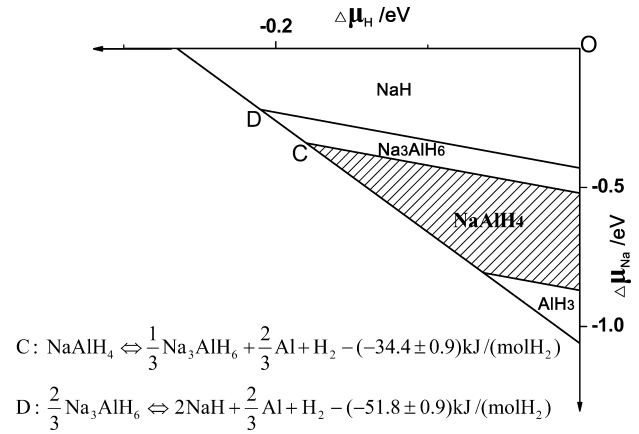

Figure 1. Chemical potential phase diagram of $NaAlH_4$. The shadowed region is the stable area of $NaAlH_4$ with points C and D corresponding to the first and second hydriding/dehydriding critical points, respectively. The reaction equations at point C and D correspond to eqs 9 and 10 in the text, respectively.

which is point C in Figure 1. At point C, $NaAlH_4$, Al, Na_3AlH_6, and H_2 coexist; thus, the reaction equation can be expressed as eq 9 which is the same as the reaction equation deduced from experiments.[7] Similarly, point D in Figure 1 is the hydriding/dedydriding critical point of the second hydriding/dehydriding step reaction, and the reaction equation is shown as eq 10 which is in accordance with experiment too.

$$NaAlH_4 \Leftrightarrow \frac{1}{3}Na_3AlH_6 + \frac{2}{3}Al + H_2 - (-34.4 \pm 0.9)\ \text{kJ/(mol}\ H_2) \quad (9)$$

$$\frac{2}{3}Na_3AlH_6 \Leftrightarrow 2NaH + \frac{2}{3}Al + H_2 - (-51.8 \pm 0.9)\ \text{kJ/(mol}\ H_2) \quad (10)$$

The reaction enthalpies of eqs 9 and 10 were obtained from the formation enthalpies calculated from eq 3 and are in agreement with reported results, which are −36 kJ/(mol H_2) and −47 kJ/(mol H_2), respectively.[33]

3.2. The Effect of Ti Additive to $NaAlH_4$.

3.2.1. The Competing Phase Introduced by Ti Additive. For the TM−Na−Al−H system, the phase equilibrium relation is also characterized by the method described above, but competing phases induced by additives should be included. We take the system of adding Ti as an example. When the appropriate amount of Ti is added, some new phases, which are competing phases to $NaAlH_4$, may be formed in the Na−Al−H−Ti system. Therefore, those new phases induced by Ti addition should be identified first.

All the possible Ti-containing phases were searched from the available databases, such as ICSD and ACS, and no Ti−Na binary phase and Ti−Na−Al−H quaternary phase were found. The formation enthalpies of all Ti−H and Ti−Al binary phases as well as Ti−Al−H ternary phase were calculated. It shows that TiH_2 is the most stable phase among the Ti−H binary phases, and $TiAl_3$ is the most stable phase among the Ti−Al binary phases. Ti_3AlH is the only ternary phase with atomic position information we could find. The solubility of H in $TiAl_3$ is low and has little influence on the chemical potential of H. Therefore, the dissolving of H in $TiAl_3$ compounds was not discussed. From above analysis, $TiAl_3$, TiH_2, and Ti_3AlH were considered as potential competition phases needed to be studied further, and their formation enthalpies are listed in Table 1.

According to the definition given before, the relative chemical potentials of the Ti is denoted as $\Delta\mu_{Ti} = \mu_{Ti} - \mu_{Ti}^{crys}$.

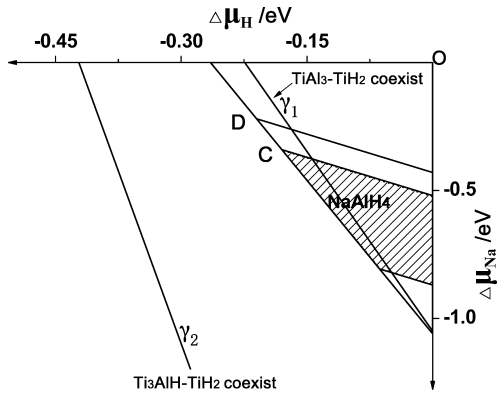

Figure 2. Critical conditions of $TiAl_3-TiH_2$ and TiH_2-Ti_3AlH coexisting. The shadowed region is the stable zone of $NaAlH_4$. Lines γ_1 and γ_2 correspond to the coexisting conditions for $TiAl_3-TiH_2$ and TiH_2-Ti_3AlH, respectively. Detailed discussion is given in the text along with eqs 15 and 16.

In principle, the competitive ability of a competing phase changes according to its chemical environment. Therefore, when the competitive ability of competition phases is compared, the chemical environment of the competing phases in SCPR of $NaAlH_4$ should be considered. The minimum $\Delta\mu_{Ti}$ required for the formation of a Ti-containing competing phase at any point in SCPR of $NaAlH_4$ can be calculated, and the phase that has smaller $\Delta\mu_{Ti}$ possesses stronger competitive ability at the chemical environment of this point. Considering that one competing phase has stronger competing ability in a certain region in SCPR of $NaAlH_4$,[34] it is only necessary to determine the boundary of those regions in which one of the competing phases has stronger competing ability. The boundary is actually a critical line along which different Ti-containing phases, such as $TiAl_3$ and TiH_2, coexist and have equal competing ability. It means that those two phases have the same $\Delta\mu_{Ti}$ along this line.

When all the kinetic barriers are neglected, the competitive ability is determined by the relationship of corresponding formation enthalpies. The formation conditions for $TiAl_3$, TiH_2 and Ti_3AlH are decided by eqs 11−13, respectively. Their formation enthalpies were also calculated and are given below:

$$\Delta\mu_{Ti} + 3\Delta\mu_{Al} = H_f(TiAl_3) = -1.59 \pm 0.01 \text{ eV} \quad (11)$$

$$\Delta\mu_{Ti} + 2\Delta\mu_{H} = H_f(TiH_2) = -1.55 \pm 0.01 \text{ eV} \quad (12)$$

$$3\Delta\mu_{Ti} + \Delta\mu_{Al} + \Delta\mu_{H} = H_f(Ti_3AlH) = -1.91 \pm 0.01 \text{ eV} \quad (13)$$

When $TiAl_3$ and TiH_2 coexist in the system, the corresponding critical chemical potentials of Ti, Al, H, and Na are expressed as$\Delta\mu_1^C(Ti)$, $\Delta\mu_1^C(Al)$, $\Delta\mu_1^C(H)$, and$\Delta\mu_1^C(Na)$. At this state, according to eqs 11 and 12, the relationship between the chemical potential and formation enthalpy of the phases is the following:

$$H_f(TiAl_3) - 3\Delta\mu_1^C(Al) = \Delta\mu_1^C(Ti) = H_f(TiH_2) - 2\Delta\mu_1^C(H) \quad (14)$$

It can be expressed with $\Delta\mu_1^C(Na)$ and $\Delta\mu_1^C(H)$ as the following:

$$3\Delta\mu_1^C(Na) + 14\Delta\mu_1^C(H) = 3H_f(NaAlH_4) - H_f(TiAl_3) + H_f(TiH_2) \quad (15)$$

According to eq 15, a line denoted as γ_1 can be drawn and is shown in Figure 2, which means that when $\Delta\mu_{Ti}$ changes, the coexisting condition of $TiAl_3$ and TiH_2 would shift along line γ_1.

Similarly, the equilibrium condition for TiH_2 and Ti_3AlH can be expressed by eq 16.

$$\Delta\mu_2^C(Na) + 9\Delta\mu_2^C(H) = H_f(NaAlH_4) - H_f(Ti_3AlH) + 3H_f(TiH_2) \quad (16)$$

According to eq 16, a line denoted as γ_2 can be drawn and is shown in Figure 2.

As shown in Figure 2, line γ_1 is across the $NaAlH_4$ stable zone, while line γ_2 locates outside of it. In fact, it is found from calculations that even at the most favorable chemical condition for the formation of Ti_3AlH, i.e., point C with the lowest $\Delta\mu_{Al}$ and the highest $\Delta\mu_H$ in SCPR of $NaAlH_4$ (c.f. Figure 1), Ti_3AlH is unstable with respect to TiH_2.

Since the competition between Ti-containing phases and $NaAlH_4$ as well as the competition among different Ti-containing phases are caused by adding Ti, the competition ability can be discussed with $\Delta\mu_{Ti}$ conveniently. When $\Delta\mu_{Ti}$ is given, the $TiH_2-NaAlH_4$ and the $TiAl_3-NaAlH_4$ coexisting conditions can be formulized as eqs 17 and 18 in the $\Delta\mu_H-\Delta\mu_{Na}$ coordinate system.

$$\Delta\mu_H = H_f(TiH_2) - \Delta\mu_{Ti} \quad (17)$$

$$\Delta\mu_{Na} + 4\Delta\mu_H = H_f(NaAlH_4) - [H_f(TiAl_3) - \Delta\mu_{Ti}]/3 \quad (18)$$

When $\Delta\mu_{Ti}$ is known, the destabilizing extent of $NaAlH_4$ could be determined by the above two equations. We take a medium value as an example to illustrate that in Figure 3a. Here line α represents the chemical condition for coexistence of $TiAl_3$ and $NaAlH_4$, and line β for coexistence of TiH_2 and $NaAlH_4$. Lines α and β intersect at point R and divide the SCPR of $NaAlH_4$ into four parts (Figure 3a). It is easy to know that point R is a critical point where $TiAl_3$, TiH_2, and $NaAlH_4$ coexist. In the green shadow region, TiH_2 is more favorable to form than $TiAl_3$ and $NaAlH_4$; $TiAl_3$ is more favorable to form than TiH_2 and $NaAlH_4$ in the blue shadow region; both $TiAl_3$ and TiH_2 are more favorable to form than $NaAlH_4$ in the red shadow region; and the black part is the new SCPR of $NaAlH_4$ after adding Ti additive. Since the SCPR of $NaAlH_4$ is reduced and the hydriding/dehydriding critical point, $\Delta\mu_H^{eq}(0\ K)$, shifts from point C to point C_{Ti} by the increase of $\Delta\mu_{Ti}$, $NaAlH_4$ is easier to be decomposed. The above results give a clear thermodynamic description for destabilization of $NaAlH_4$ by inducing of Ti-containing competing phases.

As for the red shadow region, although it is known that $NaAlH_4$ is not stable with respect to $TiAl_3$ and TiH_2, it is not discussed so far which is the competing phase ($TiAl_3$ or TiH_2). For a clear view, the red region in Figure 3a is replotted in Figure 3b, where the favorable competing phase can be decided by its minimum required $\Delta\mu_{Ti}$. The minimum $\Delta\mu_{Ti}$ required for $TiAl_3$ is $\Delta\mu'_{Ti} = H_f(TiAl_3) - 3\Delta\mu_{Al}$, and for TiH_2 is $\Delta\mu''_{Ti} = H_f(TiH_2) - 2\Delta\mu_H$. It is found that $\Delta\mu'_{Ti} < \Delta\mu''_{Ti}$ in region 1 of Figure 3b, while $\Delta\mu'_{Ti} > \Delta\mu''_{Ti}$ in region 2. This means that $TiAl_3$ is more favorable to form in region 1 of Figure 3b, while it is TiH_2 in region 2 of Figure 3b. This is understandable because Al is richer in region 1 and H is richer in region 2. In line PR, $TiAl_3$ and TiH_2 may coexist since they require the same minimum Ti chemical potential to form.

When $\Delta\mu_{Ti}$ increases, line α moves to the right side and line β moves to the left side. Thus the cross point R moves up along with line γ_1, as the $NaAlH_4$ stable region shrinks and the stable regions of $TiAl_3$ and TiH_2 expand. It is easy to know that higher

$\Delta\mu_{Ti}$ results in a smaller stable region of $NaAlH_4$. When $\Delta\mu_{Ti} = -1.26$ eV, the cross point moves to point Q (c.f. Figure 3a), where no stable region for $NaAlH_4$ exists. That $NaAlH_4$ is completely destabilized by Ti-containing phase when $\Delta\mu_{Ti} \geq -1.26$ eV. On the other hand, when $\Delta\mu_{Ti}$ decreases to $\Delta\mu_{Ti} = H_f(TiH_2) = -1.55$ eV, the cross point of line α and line β (i.e., point R) would move down to point S along line γ_1 (Figure 3b), and TiH_2 and $NaAlH_4$ coexisting line (line β) overlaps with the right boundary of the $NaAlH_4$ stable region. $TiAl_3$ and $NaAlH_4$ coexisting line (line α) would overlap with the left boundary of the $NaAlH_4$ stable region when $\Delta\mu_{Ti} = H_f(TiAl_3) = -1.59$ eV. When $\Delta\mu_{Ti}$ further decreases, there will be no Ti-containing competing compound existing but Ti defects.

According to above theoretical analysis, $TiAl_3$ has the strongest formation ability at the hydriding/dehydriding critical point C_{Ti} in Figure 3a. This is consistent with the fact that $TiAl_3$ was found after dehydriding in many experiments.[15,16] According to Figure 3a, the formation condition of TiH_2 would be reached when the $\Delta\mu_H$ increases and reaches the value marked by line β. This is also in agreement with the experiment that TiH_2 was observed after NaH, Al, and Ti powders BM under H_2 atmosphere.[21]

3.2.2. The Influence of $TiAl_3$ on Thermodynamic Properties of $NaAlH_4$. As discussed above, the hydriding/dehydriding critical point may shift from point C to point C_{Ti} (Figure 3a) when Ti is added. According to the phase equilibrium relationship, $TiAl_3$, Na_3AlH_6, and $NaAlH_4$ coexist at point C_{Ti} and the reaction can be written as eq 19, which is the first step of the hydriding/dehydriding process of $NaAlH_4$, and the reaction enthalpy was obtained the same as in section 3.1:

$$NaAlH_4 + \frac{2}{9}Ti \leftrightarrow \frac{1}{3}Na_3AlH_6 + \frac{2}{9}TiAl_3 + H_2 - (-0.6 \pm 0.9)\ \text{kJ/(mol } H_2) \quad (19)$$

Similar to point C_{Ti}, according to the phase equilibrium relation at point D_{Ti}, we have the following equation as the second step of reaction in $NaAlH_4$.

$$\frac{2}{3}Na_3AlH_6 + \frac{2}{9}Ti \leftrightarrow 2NaH + \frac{2}{9}TiAl_3 + H_2 - (-18.0 \pm 0.9)\ \text{kJ/(mol } H_2) \quad (20)$$

When Ti is added, the reaction enthalpies of the two dehydrogenation steps increase with the increment of 34.4 and 41.1 kJ/(mol H_2), respectively, comparing with those without Ti additives in eqs 9 and 10, respectively. This indicates that the dehydriding of $NaAlH_4$ becomes easier, as well as the reaction reversibility. Thus with Ti additive, the hydriding/dehydriding performance of $NaAlH_4$ is expected to be improved in principle.

In general, the hydriding/dehydriding critical point at temperature T, $P_{H_2}^{eq}(T)$, is an ideal parameter to describe hydriding/dehydriding performance of hydrides, and it corresponds to $\Delta\mu_H^{eq}(0\ K)$ at 0 K. When the amount of Ti additive is very small, say $\Delta\mu_{Ti} < H_f(TiAl_3) = -1.59$ eV, there would be no Ti-containing compounds. When the amount of Ti additive is large enough, elementary Ti phase would exist in the equilibrium system as $\Delta\mu_{Ti}$ reaches its maximum. Therefore, in general, the higher the amount of Ti additive is, the higher $\Delta\mu_{Ti}$ is and the better destabilizing ability the Ti-containing competing phase has. In principle, the destabilizing ability of $TiAl_3$, which is the competing phase in the chemical environment at point C_{Ti}, to $NaAlH_4$ matrix can be depicted as $\Delta(\Delta\mu_H^{eq}(0\ K))/(\text{mol Ti})$. However, the quantitative relation between the amount of Ti

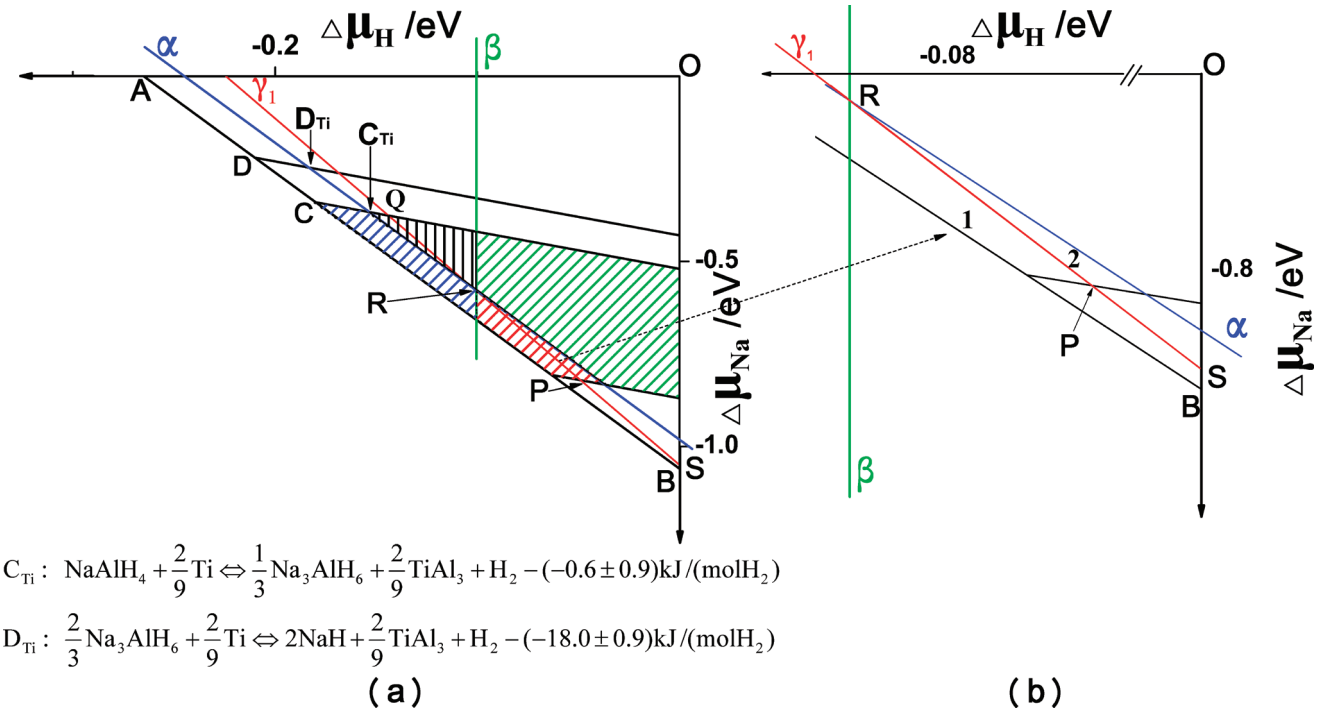

Figure 3. (a) Competition relation of $TiAl_3$ and TiH_2 in different chemical environments. Line γ_1 represents $TiAl_3-TiH_2$ coexisting condition. Lines α and β represent $TiAl_3-NaAlH_4$ and $TiH_2-NaAlH_4$ coexisting conditions, respectively. Point C and C_{Ti} are the hydriding/dehydriding critical point without and with Ti additive, respectively. The black shadow region is $NaAlH_4$ stable zone with Ti additive. (b) Detailed phase plot of the red shadow region is shown in Figure 3a. The reaction equation at point C_{Ti} and D_{Ti} corresponds to eqs 19 and 20 in the text, respectively.

TABLE 2: Formation Enthalpies of M_xAl_y and MH_z Compounds (M = Ti, V, Cr, Mn, Fe, Co, Ni, Cu, Zr, Nb, Pd, Hf)[a]

	formation enthalpies			formation enthalpies		
M_xAl_y	this work	experimental[b]	MH_z	this work	experimental	$H_f(M_xAl_y)/x$-MH_z (in this work)
$TiAl_3$	−1.59	−1.53	TiH_2	−1.55	−1.50[c], −1.34[d]	−0.04
VAl_3	−1.14	−1.16	VH_2	−0.69	−0.42[d]	−0.45
$ZrAl_3$	−1.99	−1.70	ZrH_2	−1.81	−1.75[c], −1.96[d]	−0.18
$NbAl_3$	−1.70	−1.37	NbH_2	−0.81	−0.42[d]	−0.89
Pb_8Al_{21}	−16.64		PdH	−0.21		−1.87
$HfAl_3$	−1.64	−1.74	HfH_2	−1.32	−1.34[d]	−0.32
Cr_2Al	−0.40	−0.34				
$MnAl_6$	−1.51	−1.09				
$FeAl_{3.2}$	−1.35	−1.22				
Co_2Al_9	−3.96	−3.42				
$NiAl_3$	−1.81	−1.58				
$CuAl_2$	−0.54					

[a] Unit: eV/(formula unit). [b] Reference 37. [c] Reference 35. All the experimental data of[b] and [c] are attained in the standard state of 298.15 K and 1 bar. [d] Reference 38. The data of[d] are not attained in standard state: TiH_2: <573 K; VH_2: 323−393 K; ZrH_2: 673−823 K; NbH_2: 923−1113 K; HfH_2: 873−1173 K. All the estimated uncertainties to the calculated results in this paper are 0.01 eV.

added and its chemical potential is an open question, and there is only a qualitative conclusion that a larger amount of Ti additive corresponds to a higher $\Delta\mu_{Ti}$ and a greater $\Delta\mu_H^{eq}(0\ K)$ so far. Here, we adopt $\Delta(\Delta\mu_H^{eq}(0\ K))/(\Delta\mu_{Ti})$ to describe the destabilizing ability of $TiAl_3$ to $NaAlH_4$ matrix. The bigger value of $\Delta(\Delta\mu_H^{eq}(0\ K))/\Delta\mu_{Ti}$, the stronger the destabilizing ability of $TiAl_3$ to $NaAlH_4$ matrix.

To make a semiquantitative comparison of different destabilizing ability of different TMs to $NaAlH_4$, a parameter is developed. In the precondition that the hydriding/dehydriding critical point is heightened by the same minor percentage, $c\%$, a smaller chemical potential required for M (a kind of TM) means that this kind of TM has better destabilizing ability. The parameter is symbolized with $\Delta\mu_M(c\%)$, so $\Delta\mu_M(0)$ stands for the critical value of the M-containing competing phase formation condition. Here, the increment of the hydriding/dehydriding critical point is described by a relative value instead of an absolute one for a reasonable comparison.

3.2.3. The Destabilizing Ability of TM-Containing Competing Phase to $NaAlH_4$. With the chemical potential approach described in section 3.1.2, now one is ready to study the trend of destabilizing ability of TM (M = Ti, V, Cr, Mn, Fe, Co, Ni, Cu, Zr, Nb, Pd, and Hf), among which Zr and Hf are in the same family with Ti in the periodic table; Ti, V, Cr, Mn, Fe, Co, Ni, Cu are in the same row with Ti; V, Nb are in the next family to Ti. Besides, Pd always has a great catalytic effect on decomposing H_2.

The formation enthalpies of M−Al and M−H compounds are listed in Table 2. We calculated all of the Al-containing phases and hydrides of each TM, but only the Al-containing phases and hydrides of each TM with the most superior formation ability, i.e. with the lowest chemical potential, are listed in Table 2. Among the TMs, several elements at the left side of the periodic table have stable hydrids. The TMs that have no stable hydride can only destabilize $NaAlH_4$ with their Al-containing phases. For the TMs in the same row of the periodic table of elements, $H_f(M_xAl_y)/x$-MH_z decrease from left to right (c.f. Table 2.). The situation is similar from the top to the bottom at the same family. This indicates that M_xAl_y is easier to form than MH_z as the atomic number of M increases in the same row or column. Thus, the dominating competing phases of all the TMs studied are Al rich TM−Al binary phases M_xAl_y with $x > y$, except Cr_2Al.

With the approach described in section 3.2.2, the destabilizing of those TM additives is caused by formation of competing phases which are M_xAl_y intermatallic compounds. The destabilizing ability of M_xAl_y to $NaAlH_4$ can be semiquantitatively characterized by$\Delta\mu_M(c\%)$, where $c\%$ stands for the change of $\Delta\mu_H^{eq}(0\ K)$. The destabilizing ability corresponding to $c\% = 5\%$ is shown as the line marked by open squares in Figure 4. The line marked by solid squares in Figure 4 stands for the maximum $\Delta\mu_M$ without change of $\Delta\mu_H^{eq}(0\ K)$, i.e., $c\% = 0\%$.

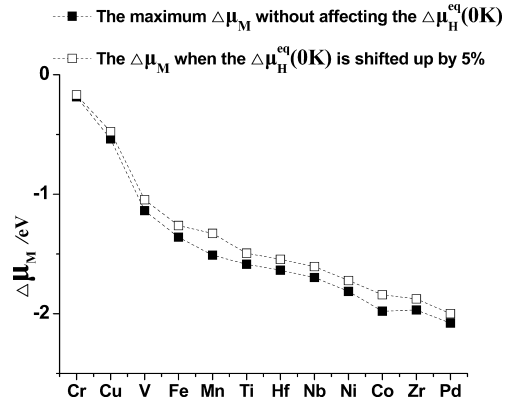

Figure 4. Destabilizing ability of M_xAl_y (M = Ti, V, Cr, Mn, Fe, Co, Ni, Cu, Zr, Nb, Pd, Hf) to $NaAlH_4$ described by the chemical potentials of TMs corresponding to different critical points. A smaller value of $\Delta\mu_M$ stands for a better destabilizing ability of M_xAl_y phase to $NaAlH_4$. Here, cases for the critical points with 0% and 5% changes with respect to the original one are shown with solid and open squares, respectively.

As shown in Figure 4, Pd_8Al_{21} has the best destabilizing effect, while Cr_2Al and $CuAl_2$ show poor effects. The destabilizing ability of M_xAl_y from low to high is $Pd_8Al_{21} > Co_2Al_9 > ZrAl_3 > NiAl_3 > NbAl_3 > HfAl_3 > TiAl_3 > MnAl_6 > FeAl_{3.2} > VAl_3 > CuAl_2 > Cr_2Al$. In general, the bigger the $H_f(M_xAl_y)/x$-value is, the stronger the destabilizing ability of M_xAl_y to $NaAlH_4$.

3.3. Experimental Dehydrogenation Kinetics of $NaAlH_4$ with Fe, Ti, and FeTi Additives. It is straightforward to verify our theory directly by adding pure TM to $NaAlH_4$. We had tried to add Ti and Fe powder in $NaAlH_4$ by ball milling. However, it is impossible to do the comparison directly since pure metal element particles are difficult to be refined by long time milling and their particle size is difficult to control in experiments because they are very ductile. Figure 5a and b are back-scattering electron SEM images of the $NaAlH_4$ milled for 20 h with Fe and Ti addition, respectively. It is found that the Fe and Ti additives are still very coarse and inhomogeneous after a long time of milling. Those coarse additives have low surface energy

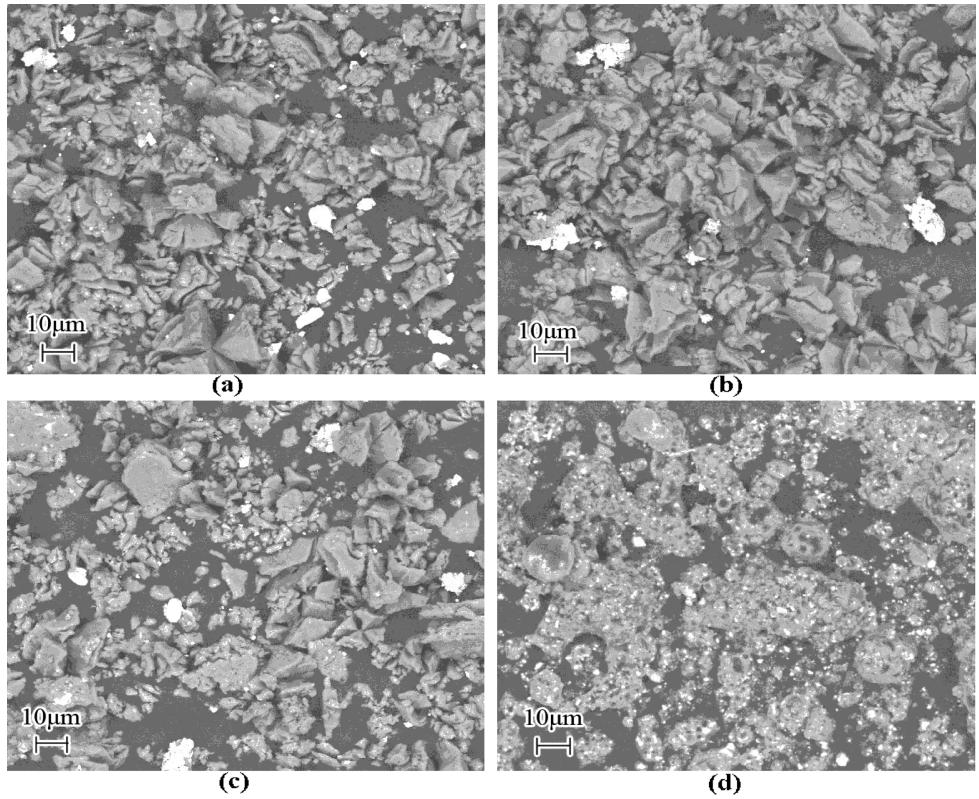

Figure 5. Back-scattering electron SEM images of specimens no. 2−5: (a) specimen no. 2, Fe-doped and milled for 20 h; (b) specimen no. 3, Ti-doped and milled for 20 h; (c) specimen no. 4, FeTi-doped and milled for 5 h; (d) specimen no. 5, FeTi-doped and milled for 20 h. The particle sizes of additives are nearly the same from the morphologies of (a), (b), and (c), while it is much smaller in (d).

and therefore relatively low reaction activity. Therefore, the difficulty in refining particles is probably the most important barrier for TMs to reach equilibrium with $NaAlH_4$ matrix and fully demonstrate their destabilizing effect on complex hydrides. This makes their destabilizing ability observed in experiment different from the theoretical predicted result. New process methods are needed to be introduced to get fine pure TMs particle to verify our theory directly.

In order to evaluate the influence of the particle size of TMs in destabilizing $NaAlH_4$, FeTi is selected as the next dopant to $NaAlH_4$ for it is a brittle intermetallic phase. It shows that the particle size of FeTi milled for 5 h, as shown in Figure 5c, is nearly the same as that of pure Fe and Ti obtained by 20 h of milling, which are shown in Figure 5a and b, respectively. The particle size of FeTi milled for 20 h, as shown in Figure 5d, is much finer than that milled for 5 h. The dehydriding kinetic curves of the $NaAlH_4$ with those different additives are given in Figure 6. It shows that the dehydriding property of $NaAlH_4$ with additive is a bit better than that without additives. When the particle size of Fe, Ti, and FeTi are nearly the same and are coarse, their destabilizing abilities have little difference. This is because the destabilized ability of additives is strongly related to their particle size, and the system cannot reach equilibrium kinetically under the experimental condition when the size of the additive is coarse. As shown in Figure 6, the FeTi alloy with fine particles (specimen no. 5) has much better destabilizing ability to $NaAlH_4$ than that of the FeTi alloy, pure Fe, and pure Ti with coarse particles. It is in accordance with the reported facts: metal element has poor ability in destabilizing complex hydrides in normal ball mill condition,[39] while the nanoparticles of Ti cluster have great destabilizing ability.[19,20] In summary, the smaller the particle size of TM, then the better the destabilizing ability to complex hydride. The possible reason

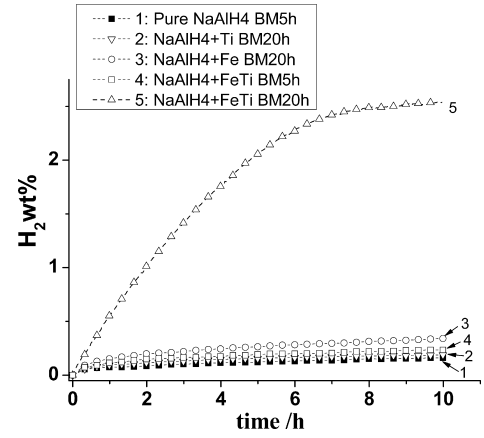

Figure 6. Isothermal dehydrogenation kinetic curves of $NaAlH_4$ with different TM additives at 393 K. The isothermal dehydrogenation kinetic curve of pure $NaAlH_4$ (specimen no. 1) under the same temperature as the reference.

is that the system is kinetically difficult to reach thermodynamic equilibrium under experimental conditions when the added additives are coarse in size.

4. Summary

In summary, we provide an alternative and convenient method to predict the influence of the TM additives to the hydriding/dehydriding of complex hydrides through the chemical potential approach. It is found that TM additives may significantly change the hydriding/dedydriding critical point of $NaAlH_4$ due to the destabilizing ability of the TM−Al competing phase. The destabilizing ability of TMs from high to low is in the following sequence: Pd > Co > Zr > Ni > Nb > Hf > Ti > Mn > Fe > V

> Cu > Cr. In comparison with the traditional chemical reaction approach, the chemical potential approach provides a straightforward and concrete description on the destabilizing ability of TMs additives. Especially, it provides information on multiphases equilibrium conditions and hydriding/dehydriding critical point, which could not be described by the traditional chemical reaction approach.

Acknowledgment. This research was supported by the NSFC under grant 50631020, Ministry of Science and Technology of China (No. 2006AA05Z126 and No. 2006AA05Z133) and the Computing resources from SCUT Grid of South China University of Technology.

References and Notes

(1) Kuijpers, F. A.; Van Mal, H. H. *J. Less-Common Met.* **1971**, *23*, 395.
(2) Li, H. W.; Ikeda, K.; Nakamori, Y.; Orimo, S.; Yakushiji, K.; Takanashi, K.; Ohyama, H.; Nakatsuji, K.; Dansui, Y. *Acta Mater.* **2007**, *55*, 481.
(3) Friedrichs, O.; Aguey-Zinsou, F.; Ares Fernández, J. R.; Sánchez-López, J. C.; Justo, A.; Klassenb, T.; Bormann, R.; Fernández, A. *Acta Mater.* **2006**, *54*, 105.
(4) Chen, D.; Wang, Y. M.; Chen, L.; Liu, S.; Ma, C. X.; Wang, L. B. *Acta Mater.* **2004**, *52*, 521.
(5) Zhu, M.; Peng, C. H.; Ouyang, L. Z.; Tong, Y. Q. *J. Alloys Compd.* **2006**, *426*, 316.
(6) Ouyang, L. Z.; Dong, H. W.; Peng, C. H.; Sun, L. X.; Zhu, M. *Int. J. Hydrogen Energy* **2007**, *32*, 3929.
(7) Bogdanovic, B.; Schwickardi, B. *J. Alloys Compd.* **1997**, *1*, 253–254.
(8) Zidan, R. A.; Takara, S.; Hee, A. G.; Jensen, C. M. *J. Alloys Compd.* **1999**, *285*, 119.
(9) Wang, T.; Wang, J.; Ebner, A. D.; Ritter, J. A. *J. Alloys Compd.* **2008**, *450*, 293.
(10) Suttisawat, Y.; Rangsunvigit, P.; Kitiyanan, B.; Muangsin, N.; Kulprathipanja, S. *Int. J. Hydrogen Energy* **2007**, *32*, 1277.
(11) Ares Fernandez, J. R.; Aguey-Zinsou, F.; Elsaesser, M.; Ma, X. Z.; Dornheim, M.; Klassen, T.; Bormann, R. *Int. J. Hydrogen Energy* **2007**, *32*, 1033.
(12) Sun, T.; Zhou, B.; Wang, H.; Zhu, M. *Int. J. Hydrogen Energy* **2008**, *33*, 2260.
(13) Sun, T.; Zhou, B.; Wang, H.; Zhu, M. *J. Alloys Compd.* **2009**, *467*, 413.
(14) Sandrock, G.; Gross, K.; Thomas, G. *J. Alloys Compd.* **2002**, *339*, 299.
(15) Sun, D. L.; Kiyobayashi, T.; Takeshita, H. T.; Kuriyama, N.; Jensen, C. M. *J. Alloys Compd.* **2002**, *337*, L8.
(16) Gross, K. J.; Guthrie, S.; Takara, S.; Thomas, G. *J. Alloys Compd.* **2000**, *297*, 270.
(17) Brinks, H. W.; Jensen, C. M.; Srinivasan, S. S.; Hauback, B. C.; Blanchard, D.; Murphy, K. *J. Alloys Compd.* **2004**, *376*, 215.
(18) Chaudhuri, S.; Graetz, J.; Ignatov, A.; Reilly, J. J.; Muckerman, J. T. *J. Am. Chem. Soc.* **2006**, *128*, 11404.
(19) Fichtner, M.; Fuhr, O.; Kircher, O. *Nanotechnology* **2003**, *14*, 778.
(20) Bogdanovic, B.; Kaskel, S.; Pommerin, A.; Schlichte, K.; Schüth, F. *Adv. Mater.* **2003**, *15*, 1012.
(21) Kang, X. D.; Wang, P.; Cheng, H. M. *J. Phys. Chem. C* **2007**, *111*, 4879.
(22) Blomqvist, A.; Araújo, C. M.; Jena, P.; Ahuja, R. *Appl. Phys. Lett.* **2007**, *90*, 141904.
(23) Liu, J. J.; Ge, Q. F. *J. Phys. Chem. B* **2006**, *110*, 25863.
(24) Marashdeh, A.; Olsen, R. A.; Løvvik, O. M.; Kroes, G. J. *J. Phys. Chem. C* **2007**, *111*, 8207.
(25) Reilly, J. J.; Wiswall, R. H. *Inorg. Chem.* **1967**, *6*, 2220.
(26) Vajo, J. J.; Skeith, S. L.; Meters, F. *J. Phys. Chem. B* **2005**, *109*, 3719.
(27) Chen, P.; Xiong, Z. T.; Luo, J. Z.; Lin, J. Y.; Tan, K. L. *Nature.* **2002**, *420*, 302.
(28) Alapati, S. V.; Johnson, J. K.; Sholl, D. S. *J. Phys. Chem. C* **2007**, *111*, 1584.
(29) Segall, M. D.; Philip, J. D. L.; Probert, M. J.; Pickard, C. J.; Hasnip, P. J.; Clark, S. J.; Payne, M. C. *J. Phys.: Condens. Matter* **2002**, *14*, 2717.
(30) Hohenberg, P.; Kohn, W. *Phys. Rev.* **1964**, *136*, B864.
(31) Kohn, W.; Sham, L. J. *Phys. Rev.* **1965**, *140*, A1133.
(32) Perdew, J. P.; Wang, Y. *Phys. Rev. B* **1992**, *45*, 13244.
(33) Orimo, S. I.; Nakamori, Y.; Jennifer, R. E.; Züttel, A.; Jensen, C. M. *Chem. Rev.* **2007**, *107*, 4111.
(34) Bai, K. W.; Wang, P. *Appl. Phys. Lett.* **2006**, *89*, 201904.
(35) *Thermochemical Data of Pure Substances*, 3rd edition; Wiley-VCH Verlag GmbH: New York, 1995.
(36) Sornadurai, D.; Panigrahi, B.; Ramani, *J. Alloys Compd.* **2000**, *305*, 35.
(37) De Boer, F. R.; Boom, R.; Mattens, W. C. M.; Miedema, A. R.; Niessen, A. K. *Cohension in Metals-Transition Metal Alloys*; North-Holland Physics Publishing Elsevier Science Publishers B. V: New York, 1988.
(38) Fukai, Y. *The Metal-Hydrogen System Basic Bulk Properties*, 2nd revised and updated edition; Springer-Verlag Berlin Heidelberg: Germany, 2005.
(39) Zheng, X. P.; Qu, X. H.; Humail, I. S.; Li, P.; Wang, G. Q. *Int. J. Hydrogen Energy* **2007**, *32*, 1141.

JP808775V